Value of multi-slice spiral computed tomography in the diagnosis of metastatic lymph nodes and N-stage of gastric cancer

**Min Jiang*, Xiaoxiao Wang*, Xiuhong Shan,
Donggang Pan, Yingjun Jia, Enzhen Ni,
Yuan Hu and Hao Huang**

Abstract

Objective: To establish new diagnostic criteria for improvement of the accuracy of multi-slice spiral computed tomography (MSCT) in diagnosing the N-stage and lymph node (LN) metastasis of gastric cancer (GC).

Methods: MSCT was performed with plain and triphasic dynamic contrast enhancement. Different regions of LN metastasis and N-staging were determined according to the herein-proposed combined diagnostic criteria and were then correlated with the pathological analysis. The Kappa consistency test was used to study the accuracy of MSCT.

Results: The accuracy of MSCT in diagnosing the N-stage as a whole was 86.3%, and that in diagnosing LN metastasis was 79.1% to 98.9%. The Kappa values for stages N0, N1, and N3 ranged from 0.449 to 0.662, indicating good consistency in diagnosing these three stages between MSCT and the postsurgical pathological results. The K_{total} value was 0.567 between MSCT and the postsurgical pathological results in diagnosing LN metastasis. The risk of LN metastasis increased with the progression of lesion infiltrates.

Conclusions: Application of the combined diagnostic criteria increased the diagnostic performance of MSCT in not only judging the N-stage but also diagnosing LN metastasis. This study will provide valuable reference data for surgical planning for patients with GC in the clinical setting.

Department of Medical Imaging, Affiliated People's Hospital of Jiangsu University, Zhenjiang, Jiangsu, China
*These authors contributed equally to this work.

Corresponding author:
Xiuhong Shan, Department of Medical Imaging, Affiliated People's Hospital of Jiangsu University, No. 8 Dianli Road, Zhenjiang City, Jiangsu Province 212002, China.
Email: xiuhongshan112@163.com

Introduction

Gastric cancer (GC) is one of the most prevalent malignant tumors.[1] Gastric carcinoma originates from gastric mucosal epithelial cells and is the most common malignant tumor in the digestive tract. The incidence of GC is higher in male than female patients. GC metastasis can be divided into three types: hematogenous spread, implantation metastasis, and lymphatic metastasis. Among these, lymphatic metastasis is the most common.[2] Correct diagnosis of the cancer stage and implementation of proper treatment (including surgical excision, palliative chemotherapy, neoadjuvant therapy, and a multimodality approach) can improve patients' survival rates. Lymph node (LN) metastasis around the stomach (Nos. 1–16) is assessed before surgery.[3–5] Among these LNs, those located at station No. 16 are not only present around the stomach but also include LNs in the aortic hiatus (16a1) and around the abdominal aorta (16a2-, b1, and b2). With the development of endoscopic submucosal dissection (ESD), increasing numbers of patients with early-stage GC who have no metastasis to LNs around the stomach are undergoing ESD treatment with less injury. Therefore, accurate preoperative diagnoses of LN metastasis and the N-stage are critical for making clinical treatment decisions and predicting the prognosis of patients with GC.

Multi-slice spiral computed tomography (MSCT), positron emission tomography–computed tomography (PET-CT), magnetic resonance imaging (MRI), and ultrasonography are commonly used imaging technologies for a clinical diagnosis of GC.[6] Ultrasonography is often the initial diagnostic method for GC; however, its accuracy is limited by the detection area and the operator's skill level, and LN inflammation can be misdiagnosed as LN metastasis.[7] The diagnostic specificity of MRI is considered satisfactory in diagnosing LN metastasis; however, MRI takes time and may produce low-resolution images.[8] The accuracy of detecting LNs around the stomach and determining the N-stage by PET-CT is better than that by enhanced CT. However, the sensitivity of PET-CT is not satisfactory in detecting LNs with diameters of <3 mm.

With the development of imaging technology, MSCT is now being used to evaluate metastasis to LNs around the stomach in the diagnosis of GC. Although the accuracy of MSCT has been improved, the diagnostic criteria still require further advancement and optimization.[9] The most commonly used clinical staging criteria for GC is the tumor-node-metastasis (TNM) staging criteria proposed by the American Joint Committee on Cancer in 2010.[10] However, nonuniform diagnostic criteria have been established for the diagnosis of the LN metastasis status around the stomach. Additionally, the diagnostic accuracy varies among different criteria. Although MSCT in combination with multiplanar reformation can clearly show the location and size of LNs, it is still difficult to distinguish metastatic LNs from inflammatory

hyperplasia of LNs. Thus, further research is needed to improve the accuracy of MSCT for diagnosing LN metastasis.

Through a combined analysis of the short-axis diameter, ratio of the short to long diameter, morphology, and CT value, our objective in this study was to evaluate and improve the diagnostic accuracy of MSCT for diagnosing both the N-stage and LN metastasis of GC.

Materials and methods

Patients

Patients with GC were recruited from January 2012 to February 2016. The inclusion criteria were a diagnosis of GC by gastroscopic biopsy, no radiotherapy or chemotherapy prior to surgery, and the performance of MSCT imaging. The exclusion criteria were a history of allergy to iodine contrast agents and the presence of other abdominal tumors. The histological diagnosis and clinical presentations were extracted from the medical records. All patients underwent MSCT examinations 2 to 7 days before undergoing surgical resection of GC. Twelve lesions were located in the gastric antrum, 4 in the gastric antrum lesser curvature, 19 in the gastric corpus lesser curvature, 6 in the gastric corpus greater curvature, 18 in the cardia, 23 in the cardia lesser curvature, and 9 in the gastric angle.

This retrospective study was approved by the institutional review board of our independent ethics committee. All patients provided informed consent before the study began.

MSCT protocol

MSCT was performed with plain and triphasic dynamic contrast enhancement before surgery using a Siemens Sensation 64 CT scanner (Siemens, Munich, Germany) and Brilliance 256-slice spiral CT scanner (Philips, Eindhoven, the Netherlands). The scanning parameters were set as follows: voltage, 120 kV; electric current, 220 to 250 mAs; and thick layer, 0.625 and 0.5 mm. All patients were examined after fasting for 8 hours. The stomach was filled with 800 to 1000 mL of warm water orally, and 20 mg of anisodamine hydrochloride (654-2) was then intramuscularly injected 10 minutes before CT scanning of the patients in the supine position. Next, a non-ionic contrast agent (Ultravist 300; Schering, Berlin, Germany) was injected into the cubital vein (iodine concentration: 270 mg/100 mL) at a rate of 3.0 mL/s and total volume of 1.5 mL/kg. Arterial-phase images were acquired 35 s after contrast injection, and venous-phase images were acquired at 70 s. The scan range extended from the top of the diaphragm to the lower edge of the liver or stomach. The scan range for assessing peritoneal spread extended from the liver dome to the pubic symphysis. After scanning, axial 3-mm soft tissue window reconstruction was performed to visualize plain, arterial-phase, and venous-phase images and determine the coronal plane and venous phase.

Combined diagnostic criteria for metastatic LNs

The anatomic locations of the LNs around the stomach and the location marks on the CT images were determined. Different groups of metastatic LNs and N-stages of GC were analyzed using the following combined diagnostic criteria: short LN diameter, ≥ 5 mm; ratio of short to long diameter, ≥ 0.7; flat CT value of ≥ 25 HU or mild/moderate enhancement (venous phase, ≥ 75 HU); or fusion of multiple LNs with none of the above conditions.

MSCT image analysis

Three radiologists in abdominal imaging retrospectively analyzed all CT images and reached a consensus. The following LN features were carefully analyzed: short diameter, ratio of short to long diameter, flat CT value or mild/moderate enhancement CT value, and LN morphology. The Kappa consistency assay was used to assess the consistency of the radiologists' assessments. Statistical analysis was performed using IBM SPSS Statistics for Windows, version 21.0 (IBM Corp., Armonk, NY, USA). The Kappa consistency test was used to assess the consistency of MSCT and the postsurgical pathological diagnostic results (as the gold standard) for metastatic LNs and the N-stage in patients with GC. Good consistency was defined as K > 0.75, fair consistency was defined as $0.40 \leq K \leq 0.75$, and poor consistency was defined as K < 0.40.

The diagnostic performance of MSCT for LN metastasis and N-staging, including the accuracy, sensitivity, and specificity, was examined by receiver operating characteristic analysis. The four-fold chi-square test and Fisher's exact probability assay were performed to compare the sensitivities of MSCT for different GC N-stages. Using the new diagnostic criteria, the χ^2 split test was used for multi-sample comparisons. A *P* value of ≤ 0.05 was considered statistically significant.

Surgery

The patients underwent radical total gastrectomy, distal gastrectomy, or proximal gastrectomy. All patients underwent lymphadenectomy.

Results

Patients and procedures

In total, 91 patients with GC were included in this study (73 men, 18 women; age range, 32–82 years; mean age, 60.6 ± 9.37 years). Among the 91 patients, 35 underwent radical total gastrectomy, 34 underwent distal gastrectomy, and 22 underwent proximal gastrectomy. All patients underwent lymphadenectomy, and 706 LNs were excised (215 metastatic and 491 nonmetastatic).

Pathological histopathology classification and diagnosis of LNs in patients with GC

According to the patients' pathological diagnosis, 34 patients were diagnosed with poorly differentiated adenocarcinoma, 2 were diagnosed with poorly differentiated adenocarcinoma with partial signet-ring cell carcinoma, 22 were diagnosed with moderately and poorly differentiated adenocarcinoma, 1 was diagnosed with moderately and poorly differentiated adenosquamous carcinoma, 26 were diagnosed with moderately differentiated adenocarcinoma, 3 were diagnosed with moderately and well-differentiated adenocarcinoma, and 3 were diagnosed with well-differentiated adenocarcinoma. According to the Lauren histotype, 51 patients had intestinal GC and 40 had diffuse-mixed GC. With respect to LN metastasis, 52 patients had no LN metastasis and 39 had LN metastasis. With respect to N-staging, 52 patients had N0 stage GC, 6 had N1 stage, 14 had N2 stage, and 19 had N3 stage.

Table 1. Consistency analysis of N-staging of gastric cancer among three physicians

Groups	K value			
	N0	N1	N2	N3
A and B	0.954	0.768	0.616	0.751
A and C	0.932	0.821	0.690	0.712
B and C	0.932	0.783	0.552	0.652

Note: A, B, and C each represents one radiologist

Analysis of N-staging consistency between pathological diagnoses

The Kappa consistency assay was used to examine the consistency between any two physicians in diagnosing the N-stage (Table 1). The results showed high consistency between physicians in diagnosing N0 and N1 stage GC. The Kappa value for N0–N3 between any two physicians ranged from 0.552 to 0.954, indicating that the three physicians had good consistency in determining the N-stage of GC.

Performance of MSCT imaging in diagnosing the N-stage

Different groups of metastatic LNs and N-stages of GC shown by MSCT images were analyzed using the combined diagnostic criteria proposed in our study. The distribution and anatomical landmarks of different groups of LNs around the stomach are shown in Figure 1. The CT manifestations of fusion of multiple metastatic LNs are shown in Figure 2. According to the MSCT imaging results, 205 LNs had a short diameter of ≥ 5 mm. The mean short diameter of the metastatic LNs was 6.58 ± 2.63 mm, and the mean short diameter of nonmetastatic LNs was 5.31 ± 1.87 mm.

The accuracy of MSCT for N-staging as a whole was 86.3%. The accuracy, sensitivity, specificity, and positive and negative predictive values of N0, N1, N2, and N3 are shown in Table 2. The consistency between MSCT imaging and the postsurgical pathological results in diagnosing the N-stage (except N2) was good, with Kappa values ranging from 0.449 to 0.662. According to $\alpha = 0.007$, we observed statistically significant differences with regards to the diagnostic sensitivity between N0 and N2 ($P = 0.007$) and between N0 and N3 ($P = 0.001$). However, no statistically significant difference was found in the accuracy

of MSCT imaging for diagnosis of the N-stage (Table 2).

Performance of MSCT imaging in diagnosing LN metastasis

According to the preoperative MSCT imaging findings, 198 patients were diagnosed with metastatic LNs and 329 patients were diagnosed with nonmetastatic LNs. During surgery, we found that 215 patients had metastatic LNs and 419 patients had nonmetastatic LNs.

As shown in Table 3, we found that the accuracy of MSCT imaging in diagnosing metastatic LNs in station No. 2 (left cardia), No. 10 (splenic hilum), and No. 13 (retropancreas) reached 98.9% and that the sensitivity for station No. 2 (left cardia), No. 9 (celiac trunk), No. 10 (splenic hilum), and No. 13 (retropancreas) was 100%. The specificity for LN station No. 2 (left cardia), No. 10 (splenic hilum), and No. 13 (retropancreas) reached 98.9%. The positive predictive value for LN station No. 3 (lesser curvature) reached 85.7%. The negative predictive value for LN station No. 2 (left cardia), No. 9 (celiac trunk), No. 10 (splenic hilum), and No. 13 (retropancreas) was 100%. The K_{total} value between MSCT imaging and the postsurgical pathological results in diagnosing metastatic LNs was 0.567. The consistency was good between MSCT imaging and the postsurgical pathological results for LN station Nos. 2, 7, 10, 11, and 13.

Association between lesion infiltration and N-staging

The association between T-staging and N-staging in patients with GC was analyzed. The results showed that 12 patients with N0 stage GC had T1a–T1b stage GC (tumor invasion to the mucosal lamina propria, mucosal muscularis, or submucosa) and that 23 patients had T2 stage GC (tumor invasion to the mucosal lamina
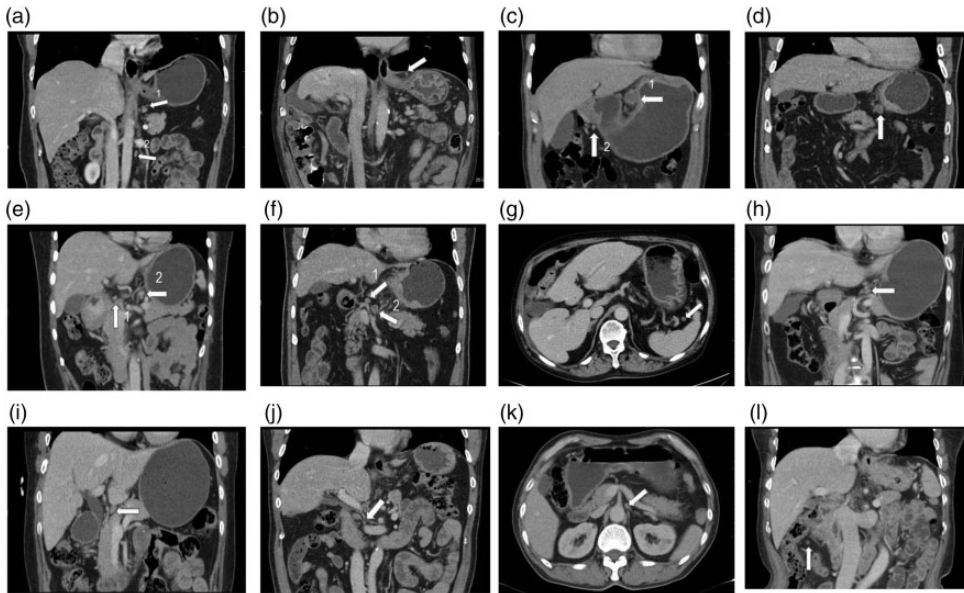
Figure 1. Distribution and anatomical landmarks of the 16 groups of lymph nodes around the stomach. (a) A 55-year-old woman with poorly differentiated adenocarcinoma in the gastric lesser curvature. Arrow 1 indicates the No. 1 right cardiac lymph nodes. Arrow 2 indicates the No. 16 para-aortic group of lymph nodes. (b) A 68-year-old man with poorly differentiated adenocarcinoma in the gastric antrum. The arrow indicates the No. 2 left cardia lymph nodes. (c) A 51-year-old man with moderately and poorly differentiated adenocarcinoma in the cardia lesser curvature. Arrow 1 indicates the No. 3 lymph nodes along the lesser curvature. Arrow 2 indicates the No. 6 intrapyloric group of lymph nodes. (d) A 69-year-old man with moderately and poorly differentiated adenocarcinoma in the cardia lesser curvature. The arrow indicates the No. 4 lymph nodes along the greater curvature. (e) A 53-year-old woman with poorly differentiated adenocarcinoma in the gastric antrum. Arrow 1 indicates the No. 5 suprapyloric group of lymph nodes. Arrow 2 indicates the No. 7 lymph nodes along the left gastric artery. (f) A 69-year-old man with poorly differentiated adenocarcinoma in the gastric antrum. Arrow 1 indicates the No. 8 lymph nodes along the common hepatic artery. Arrow 2 indicates the No. 9 lymph nodes around the celiac artery. (g) A 68-year-old man with poorly differentiated adenocarcinoma in the gastric antrum. The arrow indicates the No. 10 lymph nodes at the splenic hilum. (h) A 42-year-old woman with poorly differentiated adenocarcinoma in the gastric antrum. The arrow indicates the No. 11 lymph nodes along the splenic artery. (i) A 68-year-old woman with moderately differentiated adenocarcinoma in the gastric lesser curvature. The arrow indicates the No. 12 lymph nodes in the hepatoduodenal ligament. (j) A 64-year-old man with early-stage carcinoma in the gastric antrum. The arrow indicates the No. 13 lymph nodes behind the pancreatic head. (k) A 65-year-old man with moderately differentiated adenocarcinoma in the gastric cardia lesser curvature. The arrow indicates the No. 14 lymph nodes at the root of the mesentery or superior mesenteric artery. (l) A 68-year-old woman with moderately differentiated adenocarcinoma of the stomach. The arrow indicates the No. 15 lymph nodes along the middle colic artery

propria). However, 1 patient (about 4.3%) had N1 stage, 22 patients (about 95.7%) had N0 stage, 27 patients had T3 stage (tumor penetrating connective tissue), 4 patients (about 14.8%) had N1 stage, 6 patients (about 22.2%) had N2 stage, and 5 patients (about 18.5%) had N3 stage. Twenty-nine patients were found to have
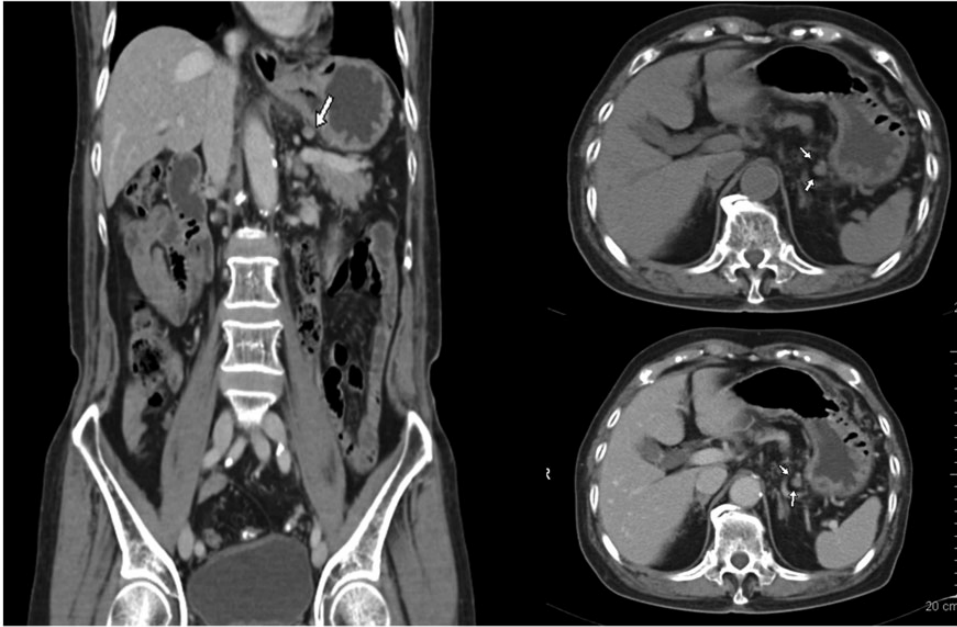
Figure 2. Computed tomography (CT) manifestations of metastatic lymph nodes. This figure shows the images of an 83-year-old man with ulcerative-type moderately differentiated canalicular adenocarcinoma in the gastric antrum. The arrow indicates the No. 1 right cardia lymph nodes. The short diameter of the lymph nodes is 6.1 mm, the flat CT value is 40.6 HU ($\geq$25 HU), and the mild/moderate enhancement CT value is 69.8 HU ($\leq$75 HU). The presence of metastasis was confirmed by pathologic examination.

Table 2. Comparison of MSCT and pathological findings in N-staging of gastric cancer.

MSCT stage	Pathological stage				Accuracy (%)	Sensitivity (%)	Specificity (%)	Positive predictive value (%)	Negative predictive value (%)	K value
	N0	N1	N2	N3						
N0	45	1	5	2	83.5 (76/91)	86.5 (45/52)	79.5 (31/39)	84.9 (45/53)	81.6 (31/38)	0.662
N1	5	5	2	2	89.0 (81/91)	83.3 (5/6)	89.4 (76/85)	35.7 (5/14)	98.7 (76/77)	0.449
N2	2	0	7	6	83.5 (76/91)	50.0 (7/14)	89.6 (69/77)	46.7 (7/15)	90.8 (69/76)	0.385
N3	0	0	0	9	89.0 (81/91)	47.4 (9/19)	100.0 (72/72)	100.0 (9/9)	87.8 (72/82)	0.587

MSCT, multi-slice spiral computed tomography.

T4a–T4b stage GC (tumor invasion of serous or adjacent tissue structures), 2 patients (about 6.9%) had N1 stage, 7 patients (about 24.1%) had N2 stage, and 14 patients (about 48.3%) had N3 stage. These results indicate that with the progression of lesion infiltration, the risk of LN metastasis increases (Table 4).

Table 3. MSCT evaluation of metastatic lymph nodes in 91 patients with gastric cancer.

MSCT lymph nodes		Pathology Positive/Negative	Accuracy (%)	Sensitivity (%)	Specificity (%)	Positive predictive value (%)	Negative predictive value (%)	K value
No. 1 (right cardia)	Positive	9/4	90.1 (82/91)	64.3 (9/14)	94.8 (73/77)	69.2 (9/13)	93.6 (73/78)	0.609
	Negative	5/73						
No. 2 (left cardia)	Positive	2/1	98.9 (90/91)	100 (2/2)	98.9 (88/89)	66.7 (2/3)	100 (88/88)	0.795
	Negative	0/88						
No. 3 (lesser curvature)	Positive	24/4	79.1 (72/91)	61.5 (24/39)	92.3 (48/52)	85.7 (24/28)	76.2 (48/63)	0.558
	Negative	15/48						
No. 4 (greater curvature)	Positive	3/4	93.4 (85/91)	60.0 (3/5)	95.3 (82/86)	42.9 (3/7)	97.6 (82/84)	0.466
	Negative	2/82						
No. 5 (suprapyloric)	Positive	0/2	97.8 (89/91)	–	97.8 (89/91)	–	–	–
	Negative	0/89						
No. 6 (infrapyloric)	Positive	3/5	93.4 (85/91)	75.0 (3/4)	94.3 (82/87)	37.5 (3/8)	98.8 (82/83)	0.469
	Negative	1/82						
No. 7 (left gastric artery)	Positive	7/5	93.4 (85/91)	87.5 (7/8)	94.0 (78/83)	58.3 (7/12)	98.7 (78/79)	0.665
	Negative	1/78						
No. 8 (common hepatic artery)	Positive	3/11	84.6 (77/91)	50.0 (3/6)	87.1 (74/85)	21.4 (3/14)	96.1 (74/77)	0.229
	Negative	3/74						
No. 9 (celiac artery)	Positive	2/3	96.7 (88/91)	100 (2/2)	96.6 (86/89)	40.0 (2/5)	100 (86/86)	0.558
	Negative	0/86						
No. 10 (splenic hilum)	Positive	1/1	98.9 (90/91)	100 (1/1)	98.9 (89/90)	50.0 (1/2)	100 (89/89)	0.662
	Negative	0/89						
No. 11 (splenic artery)	Positive	3/2	96.7 (88/91)	75.0 (3/4)	97.7 (85/87)	60.0 (3/5)	95.3 (85/86)	0.650
	Negative	1/85						
No. 12 (hepatoduodenal ligament)	Positive	2/7	91.2 (83/91)	66.7 (2/3)	92.0 (81/88)	22.2 (2/9)	98.8 (81/82)	0.299
	Negative	1/81						
No. 13 (behind pancreatic head)	Positive	1/1	98.9 (90/91)	100 (1/1)	98.9 (89/90)	50.0 (1/2)	100 (89/89)	0.662
	Negative	0/89						

MSCT, multi-slice spiral computed tomography

$K_{total} = 0.567$. This value did not include data of lymph node station Nos. 14, 15, and 16 because these stations contained only one or no positive cases and are not shown in Table 3 (1 case in No. 14, no cases in No. 15, and 1 case in No. 16).

Table 4. Relationship between T-stage and N-stage of gastric cancer.

T-stage	N-stage			
	N0	N1	N2	N3
T1a–T1b	12 (100.0)	0 (0.0)	0 (0.0)	0 (0.0)
T2	22 (95.7)	1 (4.3)	0 (0.0)	0 (0.0)
T3	12 (44.5)	4 (14.8)	6 (22.2)	5 (18.5)
T4a–T4b	6 (20.7)	2 (6.9)	7 (24.1)	14 (48.3)

Data are presented as n (%).

Discussion

LN metastasis plays a critical role in affecting the prognosis of GC.[11] Although the 5-year survival rate among patients with N0 stage GC is >86.1%, this rate falls to 58.1%, 23.3%, and 5.9% for patients with N1, N2, and N3 stage GC, respectively.[12] Therefore, determining the N-stage of the LNs in patients with GC is critical for establishing optimized clinical treatment plans.

Ultrasound, MRI, and PET-CT can be used to help diagnose metastatic LNs. However, these technologies also have certain limitations. For example, the detection range of ultrasound is limited by the technology itself,[13] possibly affecting its accuracy in diagnosing diseases. Additionally, MRI examination is time-consuming,[14] which might affect the image quality and diagnostic accuracy. Furthermore, PET-CT is not sensitive to preoperative N-staging.[15] MSCT has recently been used in the diagnosis of metastatic LNs around the stomach in patients with GC. Nevertheless, MSCT imaging has lacked uniform diagnostic criteria until now.[16] The accuracy of MSCT in diagnosing LN metastasis reportedly ranges from 71.1% to 81.4% when the criterion was set as a short diameter of ≥6 mm for LNs around stomach or ≥8 mm for LNs outside the stomach.[17,18] However, some LNs with short diameters can still metastasize. Thus, the diagnostic performance can be affected by a single diagnostic parameter. On the basis of these investigations, we proposed the following new set of combined diagnosis criteria for diagnosing LN metastasis and the N-stage of GC: short LN diameter, ≥5 mm; ratio of short to long diameter, ≥0.7; flat CT value, ≥25 HU or mild/moderate enhancement (venous phase, ≥75 HU); or fusion of multiple LNs without the above symptoms. Our study showed that by using these combined diagnostic criteria, preoperative MSCT imaging had good performance in diagnosing the N-stage and LN metastasis in patients with GC with respect to accuracy, sensitivity, and specificity. Our results showed that the accuracy of N-staging as a whole was 86.3% and that of stages N0, N1, N2, and N3 was 83.5%, 89.0%, 83.5%, and 89.0%, respectively. Compared with previous studies, the present study showed improved accuracy of MSCT for diagnosis of the N-stage.[17,18] The sensitivity for N0, N1, N2, and N3 was 86.5%, 83.3%, 50.0%, and 47.4%, respectively, while the differences in the sensitivity between N0 and N2 (P = 0.007) and between N0 and N3 (P = 0.001) were statistically significant (α = 0.007). The sensitivities of N2 and N3 were lower than those of N0 and N1. The consistency between the preoperative N2 stage and the postoperative pathological diagnosis was poor (K = 0.385). Size, morphology, and the CT value are similar between inflammatory LN hyperplasia and LN metastasis, making it difficult to use CT. Thus, we cannot conclude that the sensitivity of MSCT in diagnosing stage N2/N3 GC is lower than that that in diagnosing stage N1 GC.

Identifying LN metastasis is of importance when planning operative lymphadenectomy.[19,20] Accurate assessment of LN metastasis could reduce blindness during surgery. Because ESD can be used to treat early GC, radical D2 resection is still used for most patients. Precise preoperative assessment of LN metastasis plays a vital

role in surgical planning.[21,22] Therefore, we also analyzed the diagnostic performance of MSCT in assessing LN metastasis in this study. The results showed that the accuracy of MSCT in diagnosing LN metastasis of station No. 2 (left cardia), No. 10 (hilum of spleen), and No. 13 (retropancreas) reached 98.9%. The positive predictive value in diagnosing LN metastasis in station No. 3 (lesser curvature) was as high as 85.7%, although the accuracy was as low as 79.1%. Accurate judgment regarding LN metastasis might depend on the clarity of the anatomic structures. Thus, it was difficult to distinguish metastatic LNs from inflammatory hyperplastic LNs, and this difficultly might affect the diagnostic accuracy to some extent. Good consistency was observed between preoperative MSCT imaging and the postoperative pathological diagnosis of LN metastasis at station Nos. 2, 7, 10, 11, and 13 ($K = 0.795$, 0.665, 0.662, 0.650, and 0.662, respectively), while the consistency at No. 8 ($K = 0.229$) and No. 12 ($K = 0.299$) was poor. The low accuracy in diagnosing LN metastasis at Nos. 8 and 12 may be explained by the complicated anatomic structure of the porta hepatis, which resulted in CT imaging of iconic anatomic structures (such as the hepatic artery, portal vein, and bile duct) in low resolution.

We also found an increased risk of LN metastasis as the T-stage increased. Although no apparent LN metastasis around the stomach was identified among the 12 patients with T1 GC in this study, the possibility that no LN metastasis had ever occurred around the stomach in patients with stage T1 GC could not be completely excluded because the total number of patients was small. Thus, investigating larger numbers of samples or samples from multiple centers is necessary to further study the diagnostic performance of MSCT.

In conclusion, when we applied the herein-described combined diagnostic criteria, MSCT displayed high accuracy for determining the preoperative N-stage and metastasis of various groups of LNs in patients with GC. Our results provide a valuable reference for clinical surgical planning and operative lymphadenectomy. However, although MSCT is used to determine the preoperative N-stage of GC,[23] enhanced CT examination is not applicable to patients with renal insufficiency, patients with an allergy to contrast agents containing iodine, pregnant women, and patients who need to avoid radiation exposure.[24] For such patients, diffusion-weighted MRI could be used as an alternative to MSCT to diagnose the N-stage and LN metastasis.[25–27] Thus, it could be argued that MSCT in combination with diffusion-weighted MRI could be an effective diagnostic method in diagnosing LN metastasis of GC.

Declaration of conflicting interest

The authors declare that there is no conflict of interest.

References

1. Lee S, Son T, Kim HI, et al. Status and prospects of robotic gastrectomy for gastric cancer: our experience and a review of the literature. *Gastroenterol Res Pract* 2017; 2017: 7197652.
2. Sydiuk A. Current practice for gastric cancer treatment in Ukraine. *Transl Gastroenterol Hepatol* 2017; 2: 47.
3. Son SY, Kong SH, Ahn HS, et al. The value of N staging with the positive lymph node ratio, and splenectomy, for remnant gastric

cancer: a multicenter retrospective study. *J Surg Oncol* 2017; 116: 884–893.

4. Li SM, Li ZY and Ji X. [Clinical characteristics of lymph node metastasis in Siewert type II adenocarcinoma of the gastroesophageal junction]. *Zhonghua Zhong Liu Za Zhi* 2013; 35: 288–291[in Chinese, English Abstract].

5. Japanese Gastric Cancer Association. Japanese classification of gastric carcinoma: 3rd English edition. *Gastric Cancer* 2011; 14: 101–112.

6. Holda MK, Koziej M, Wszolek K, et al. Left atrial accessory appendages, diverticula, and left-sided septal pouch in multi-slice computed tomography. Association with atrial fibrillation and cerebrovascular accidents. *Int J Cardiol* 2017; 244: 163–168.

7. He X, Sun J, Huang X, et al. Comparison of oral contrast-enhanced transabdominal ultrasound imaging with transverse contrast-enhanced computed tomography in preoperative tumor staging of advanced gastric carcinoma. *J Ultrasound Med* 2017; 36: 2485–2493.

8. Boesen L, Norgaard N, Logager V, et al. A prospective comparison of selective multiparametric magnetic resonance imaging fusion-targeted and systematic transrectal ultrasound-guided biopsies for detecting prostate cancer in men undergoing repeated biopsies. *Urol Int* 2017; 99: 384–391.

9. Jia GS, Feng GL, Li JP, et al. Using receiver operating characteristic curves to evaluate the diagnostic value of the combination of multislice spiral CT and alpha-fetoprotein levels for small hepatocellular carcinoma in cirrhotic patients. *Hepatobiliary Pancreat Dis Int* 2017; 16: 303–309.

10. Allen PJ, Kuk D, Castillo CF, et al. Multi-institutional validation study of the American Joint Commission on Cancer (8th edition) changes for T and N staging in patients with pancreatic adenocarcinoma. *Ann Surg* 2017; 265: 185–191.

11. Siewert JR, Bottcher K, Stein HJ, et al. Relevant prognostic factors in gastric cancer: ten-year results of the German gastric cancer study. *Ann Surg* 1998; 228: 449–461.

12. Chon SH, Berlth F, Plum PS, et al. Gastric cancer treatment in the world: Germany. *Transl Gastroenterol Hepatol* 2017; 2: 53.

13. Anderson NG, Warfield SK, Wells S, et al. A limited range of measures of 2-D ultrasound correlate with 3-D MRI cerebral volumes in the premature infant at term. *Ultrasound Med Biol* 2004; 30: 11–18.

14. Bliddal H, Boesen M, Christensen R, et al. Imaging as a follow-up tool in clinical trials and clinical practice. *Best Pract Res Clin Rheumatol* 2008; 22: 1109–1126.

15. Youn SH, Seo KW, Sang HL, et al. 18F-2-Deoxy-2-Fluoro-D-glucose positron emission tomography: computed tomography for preoperative staging in gastric cancer patients. *J Gastric Cancer* 2012; 12: 179–186.

16. Dai CL, Yang ZG, Xue LP, et al. Application value of multi-slice spiral computed tomography for imaging determination of metastatic lymph nodes of gastric cancer. *World J Gastroenterol* 2013; 19: 5732–5737.

17. Pan Z, Zhang H, Yan C, et al. Determining gastric cancer resectability by dynamic MDCT. *Eur Radiol* 2010; 20: 613–620.

18. Yan C, Zhu ZG, Yan M, et al. Value of multidetector-row computed tomography in the preoperative T and N staging of gastric carcinoma: a large-scale Chinese study. *J Surg Oncol* 2009; 100: 205–214.

19. Gagarina NV, Levkin VV, Fominykh EV, et al. [Capacities of diagnostic volumetric multislice spiral computed tomography in the diagnosis of gastric cancer]. *Vestn Rentgenol Radiol* 2011;(4):37–41[in Russian, English Abstract].

20. Marrelli D, Mazzei MA, Pedrazzani C, et al. High accuracy of multislices computed tomography (MSCT) for para-aortic lymph node metastases from gastric cancer: a prospective single-center study. *Ann Surg Oncol* 2011; 18: 2265–2272.

21. Martin Sanchez M, Perez Escutia MA, Lora Pablos D, et al. Adjuvant radiochemotherapy in locally advanced gastric cancer: treatment results and analysis of possible prognostic factors. *Strahlenther Onkol* 2017; 193: 1005–1013.

22. Park TG, Yu YD, Park BJ, et al. Implication of lymph node metastasis

detected on 18F-FDG PET/CT for surgical planning in patients with peripheral intrahepatic cholangiocarcinoma. *Clin Nucl Med* 2014; 39: 1–7.

23. Kim JI, Kim YH, Lee KH, et al. Type-specific diagnosis and evaluation of longitudinal tumor extent of Borrmann type IV gastric cancer: CT versus gastroscopy. *Korean J Radiol* 2013; 14: 597–606.

24. Makino T, Fujiwara Y, Takiguchi S, et al. Preoperative T staging of gastric cancer by multi-detector row computed tomography. *Surgery* 2011; 149: 672–679.

25. Giganti F, De Cobelli F, Canevari C, et al. Response to chemotherapy in gastric adenocarcinoma with diffusion-weighted MRI and (18) F-FDG-PET/CT: correlation of apparent diffusion coefficient and partial volume corrected standardized uptake value with histological tumor regression grade. *J Magn Reson Imaging* 2014; 40: 1147–1157.

26. Liu S, He J, Guan W, et al. Preoperative T staging of gastric cancer: comparison of diffusion- and T2-weighted magnetic resonance imaging. *J Comput Assist Tomogr* 2014; 38: 544–550.

27. Arslan H, Fatih Ozbay M, Calli I, et al. Contribution of diffusion weighted MRI to diagnosis and staging in gastric tumors and comparison with multi-detector computed tomography. *Radiol Oncol* 2017; 51: 23–29.